

FeCoNiMnCr high-entropy alloys (HEAs): Synthesis, structural, magnetic and nuclear radiation absorption properties



Telem Şimşek ^a, Esra Kavaz ^b, Ömer Güler ^c, Tuncay Şimşek ^d, Barış Avar ^e, Naim Aslan ^c, Ghada Almisned ^f, Hesham M.H. Zakaly ^{g,h,*}, H.O. Tekin ^{i,j}

^a Nanotechnology and Nanomedicine Division, Institute of Science, Hacettepe University, Ankara, 06800, Turkey

^b Department of Physics, Faculty of Sciences, Ataturk University, 25240, Erzurum, Turkey

^c Munzur University, Rare Earth Elements Application and Research Center, 62000, Tunceli, Turkey

^d Department of Mechanical and Metal Technologies, Kirikkale Vocational High School, Kirikkale University, 71450, Kirikkale, Turkey

^e Metallurgical and Material Engineering, Zonguldak Bülent Ecevit University, Zonguldak, Turkey

^f Department of Physics, College of Science, Princess Nourah Bint Abdulrahman University, P.O. Box 84428, Riyadh, 11671, Saudi Arabia

^g Physics Department, Faculty of Science, Al-Azhar University, Assiut, 71524, Egypt

^h Institute of Physics and Technology, Ural Federal University, Yekaterinburg, 620002, Russia

ⁱ Department of Medical Diagnostic Imaging, College of Health Sciences, University of Sharjah, 27272, Sharjah, United Arab Emirates

^j Istinye University, Faculty of Engineering and Natural Sciences, Computer Engineering Department, Istanbul, 34396, Turkey

ARTICLE INFO

Handling Editor: Dr P. Vincenzini

Keywords:

High entropy alloys
Structural properties
Magnetic properties
Nuclear radiation
Shielding materials

ABSTRACT

We report the synthesis and structural, magnetic and Radiation shielding properties of High Entropy Alloy (HEA) produced through mechanical alloying method. Using an X-Ray Diffractometer (PanalyticalEmpryan) with CuK radiation at 45 kV and 40 mA, the phase identification starting elements and as-milled powders are identified. Scanning electron microscopy (SEM) equipped with energy dispersive X-ray spectroscopy (EDX), morphological and microstructural investigations were conducted (FEI Quanta FEG 450). EDX and elemental mapping analyses are conducted to assess the purity and elemental distributions of the synthesized alloys. Using the Quantum Design Physical Characteristics Measurement System (PPMS) with vibrating sample magnetometer (VSM) and a magnetic field of 30 kOe at room temperature, magnetic properties are examined. Using ¹³⁷Cs radioisotope and mathematical methods, gamma-ray and neutron shielding properties of HEA are investigated in a conventional transmission setup using experimental and theoretical approaches. In the presence of a 3 T applied field, the sample exhibits a low magnetization of 5.30 emu/g at 300 K. Moreover, Ms is raised to 22 emu/g at 10 K owing to decreased thermal effects. The temperature dependence of the magnetization is recorded in the presence of a 1 T applied field. HEA exhibits superior neutron attenuation properties than conventional absorption materials such as B₄C, graphite, and water. Our results showed that the synthesized HEA has superiority over other alloys and conventional neutron absorption materials. It can be concluded that the proposed novel HEA might be investigated further in terms of broadening its characterization and clarifying its other crucial properties to extend the scope of the current investigation.

1. Introduction

Since the discovery of alloys until the 21st century, alloying has been focused on the addition of modest amounts of numerous different metals to a single base metal [1]. Previously, Yeh et al. [2], proposed a novel alloy idea. According to this new alloy concept, the alloy to be developed would have five or more primary elements, with the ratio of these alloying components varying between from 5% to 35% [3]. This alloy

concept has not been proposed for decades, for the most part, due to conventional metallurgical understanding. Classical metallurgical knowledge states that the greater the number of alloying elements in multicomponent alloy systems, the greater the probability of developing a variety of phases and intermetallic compounds [4]. However, this was not the situation with the alloying hypothesis presented by Yeh et al. Multiple elements mixed in proper proportions provide a high mixing entropy, and because of this entropy, one or two solid solution structures

* Corresponding author. Institute of Physics and Technology, Ural Federal University, Yekaterinburg, 620002, Russia.

E-mail addresses: h.m.zakaly@gmail.com, h.m.zakaly@azhar.edu.eg (H.M.H. Zakaly).

with a simple crystalline structure predominate in the alloy [5–7]. In recent years, this alloy type has managed to attract the interest of several researchers. This new category of materials is known as high entropy alloys (HEA). HEAs have extremely high tensile strength and ductility [8–10]. In addition, it has microstructural and mechanical stability at high temperatures, as well as exceptional wear, corrosion, and oxidation resistance [11–16].

Meanwhile, gamma radiation is a part of the electromagnetic radiation spectrum with a certain number of vibrations produced by the collision of subatomic particles. Although gamma photons are neutral, the photoelectric effect and the Compton effect [17] enable them to ionize atoms directly. They move at the speed of light and may travel hundreds of meters in the air before releasing their energy. They are capable of readily penetrating materials and passing through the human body. As it slows down and distributes its energy to the surrounding cells, it may harm living biological cells. The presence of gamma radiation necessitates the use of shielding materials, which are typically high-density materials [17–19].

On the other hand, Lead (Pb) is a substance that has these characteristics and has been used in radiation shielding applications for decades. Due to the harm to the environment caused by its toxic nature and several disadvantageous material properties [20], there was an important incentive to investigate other materials for Radiation shielding applications. Examining the studies in the scientific literature indicates that HEAs have a place in advanced nuclear technology applications and are being studied for multiple purposes. The increased compositional flexibility provided by high-entropy alloys (HEAs) presents a unique opportunity for designing alloys for advanced nuclear applications, especially in situations where conventional engineering alloys fail in some respects [21]. On the other hand, experiments at room temperature revealed that irradiated HEAs exhibit excellent phase stability and resistance to amorphization [22–25]. Expanding the studies in the scientific literature and undertaking the characterization procedures for various types of HEAs would speed up the integration of these promising materials in the nuclear industry. This work produced a high entropy FeCoNiMnCr alloy through the mechanical alloying method. In addition to examining the physical, structural, and magnetic properties, the Radiation shielding characteristics of the FeCoNiMnCr HEA alloy were also investigated. The results of this study may be useful for understanding the critical material properties and behaviors of the FeCoNiMnCr HEA sample for its utilization potential in nuclear reactors and other nuclear power components such as pipes and other body materials. As a consequence of comprehensive comparison, it may also be possible to better understand the differences in material properties between the produced HEA and other alloys.

2. Materials and methods

2.1. Synthesis and experimental procedures

In this study, Fe (Riedel-de Haen), Ni (Merck), Co (Merck), Mn (Aldrich) and Cr (Aldrich) with a purity of >99% were used as starting elements in powder form for the synthesis of FeCoNiMnCr high entropy alloy. Next, mechanical alloying experiments were performed by a high energy ball mill (Retsch PM100) under an Argon atmosphere. The sample weighing and preparation were performed in an Ar-filled Glove-Box. The ball-to-powder ratio was 10:1 and rotating speed was fixed to 400 rpm. The 250 ml hardened steel vial and 8- and 10-mm diameter hardened steel balls were utilized. Experiments were conducted for up to 30 h. To prevent excessive heat and boost productivity, the mill's rotation direction was changed every 30 min and halted for 15 min. Using an X-Ray Diffractometer (PanalyticalEmpryan) through CuK radiation at 45 kV and 40 mA, the phase identification starting elements and as-milled powders were identified, respectively. Using the well-known Williamson-Hall technique [26], the mean crystallite size and lattice strain were computed. Using scanning electron microscopy (SEM)

equipped with energy dispersive X-ray spectroscopy (EDX), morphological and microstructural investigations were conducted (FEI Quanta FEG 450). In this study, EDX and elemental mapping analyses were conducted to assess the purity and elemental distributions of the synthesized alloys. Using the Quantum Design Physical Characteristics Measurement System (PPMS) with vibrating sample magnetometer (VSM) and a magnetic field of ± 30 kOe at room temperature, magnetic properties were examined. The magnetothermal response of the nanocrystal samples was evaluated using an Ambrell Easy Heat L1 RF signal generator and a Neoptix fiber optic temperature sensor in the presence of a 300 kHz, 400 Oe AC magnetic field. The samples were ultrasonically dispersed in isopropyl alcohol before measurement.

2.2. Gamma-ray and neutron transmission measurements

Transmission equipment may be used to examine the attenuation characteristics of materials against ionizing Radiation in the most fundamental sense. This transmission mechanism may be understood by analyzing the quantitative differences between primary and secondary Radiation produced by placing the examined attenuation material between a radioactive source and a detector. Using two different experimental settings (see Figs. 1 and 2), the gamma-ray attenuation characteristics of the synthesized high entropy alloy against gamma rays and neutrons were examined in this work. All additional technical information, including test sets, radioactive isotopes, and counting principles, may be found in our previous studies [27]. First, the linear attenuation coefficients (μ , cm^{-1}) for gamma-ray attenuation parameters were determined. Next, the mass attenuation coefficients (μ_m , cm^2/g) were determined using μ values for nine discrete gamma-ray energies emitted from ^{133}Ba point isotropic radioactive source. The dose change was quantitatively studied through $^{241}\text{Am}/\text{Be}$ neutron source for the neutron attenuation characteristics of HEA. In addition, the gamma-ray and neutron attenuation characteristics are compared to those of various kinds of alloys and conventional neutron moderators previously reported in the literature.

3. Results and discussions

3.1. Structural, physical, and magnetic properties

Fig. 3 depicts the XRD pattern of the elements used as starting powders to create the FeCoNiMnCr high entropy alloy. Clearly, the peak intensities associated with the crystalline phases of Fe (ICDD Card: 87-0721, cubic, Im-3m), Co (ICDD Card: 05-0727, hexagonal, P_{63}/mmc), Ni (ICDD Card: 04-0850, cubic, Fm-3m), Mn (ICDD Card: 33-0887, cubic, $P4_132$), and Cr (ICDD Card: 06-0694, cubic, Im-3m) are bereft of any undesirable phases. **Fig. 4** depicts the XRD patterns of the 30 h as-milled high entropy FeCoNiMnCr alloy. It was observed that mechanical alloying of original materials produced a single solid solution phase of high entropy FeCoNiMnCr alloy. The XRD examination reveals that the FCC was achieved without any intermetallic structure. At the conclusion of milling, the elements Fe, Co, Mn, and Cr were infused and dissolved into the Ni lattice to produce an FCC phase. The crystallite size and lattice strain of the original powders determined using Williamson-Hall equations from the XRD data are around 107.3 nm and 0.095%, respectively. The crystallite size and lattice strain of powders milled for 30 h were calculated to be around 10.1 nm and 0.934%, respectively. Meanwhile, 3.6403 Å was observed to be the lattice parameter. As the milling time was extended to 30 h and the crystallite size was substantially reduced, the lattice strain increased owing to mechanical deformations. Initial elements encountered continuous and persistent fracturing, flattening, cold-welding, and refracting throughout the mechanical alloying procedure. Consequently, crystallite size decreased, while the structural defects such as dislocations, vacancies, and grain boundaries cause lattice strain increased [28,29]. Using SEM and EDS analysis, the morphology and



Fig. 1. HEA- Alloy sample and experimental scheme for gamma ray transmission measurements.

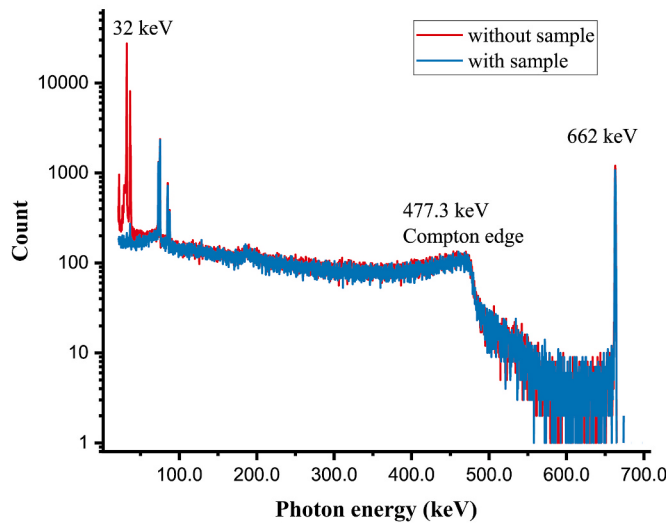
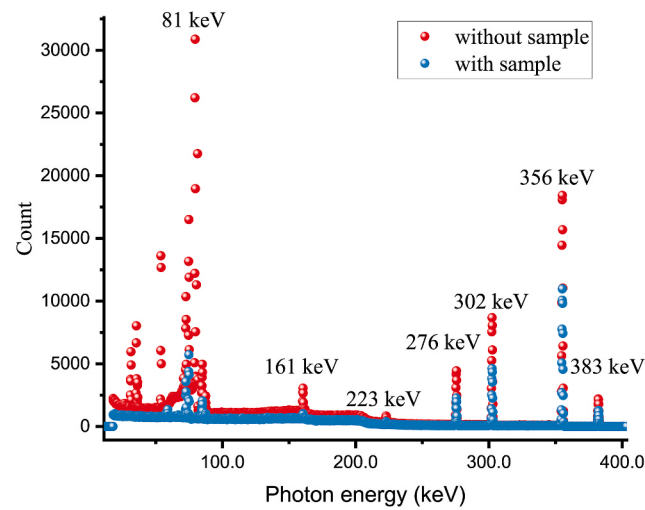


Fig. 2. Transmission spectra for Ba-133 and Cs-137 radioactive sources.

purity of the as-milled powders were also analyzed. The spherical and irregular form and morphology of the milled FeCoNiMnCr high entropy alloy are shown in Fig. 5 as SEM images. The particle size distributions become more uniform and spherical following the continuous fracturing, cold-welding, and re-fracturing of powders during mechanical alloying [28]. Fig. 6 shows the elemental mapping and EDX analysis. In

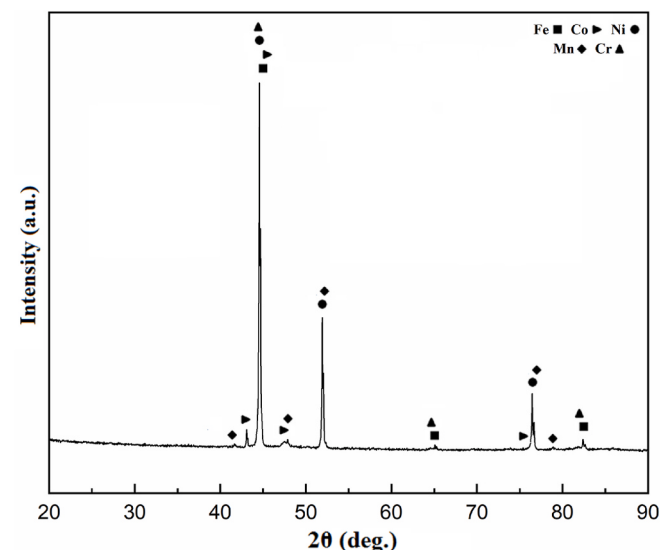


Fig. 3. XRD pattern of the initial powders.

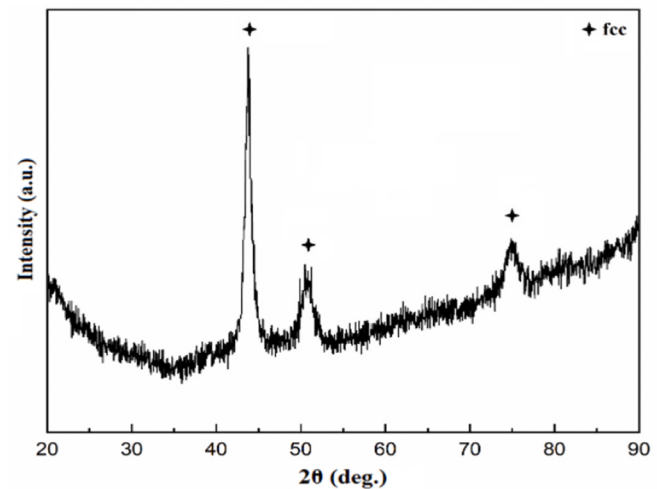


Fig. 4. XRD graphs of the 30 h as-milled FeCoNiMnCr high entropy alloy.

the high entropy alloy, elemental mapping images demonstrate homogeneous and uniform distributions of Fe, Co, Ni, Mn, and Cr elements. In addition, the EDX analysis verifies the absence of contamination from

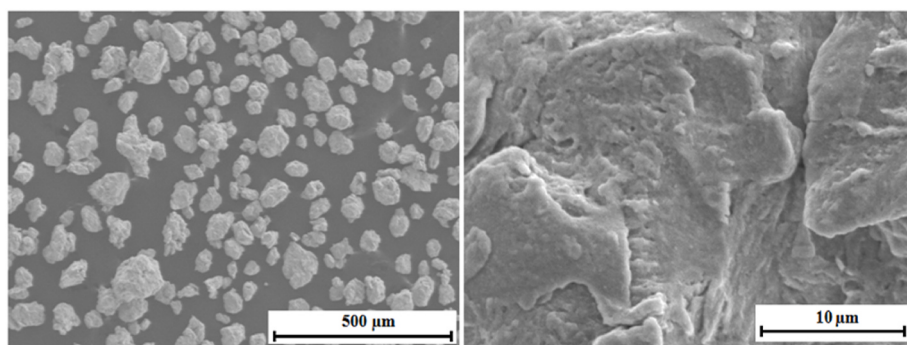


Fig. 5. SEM images of the mechanically alloyed FeCoNiMnCr high entropy alloy.

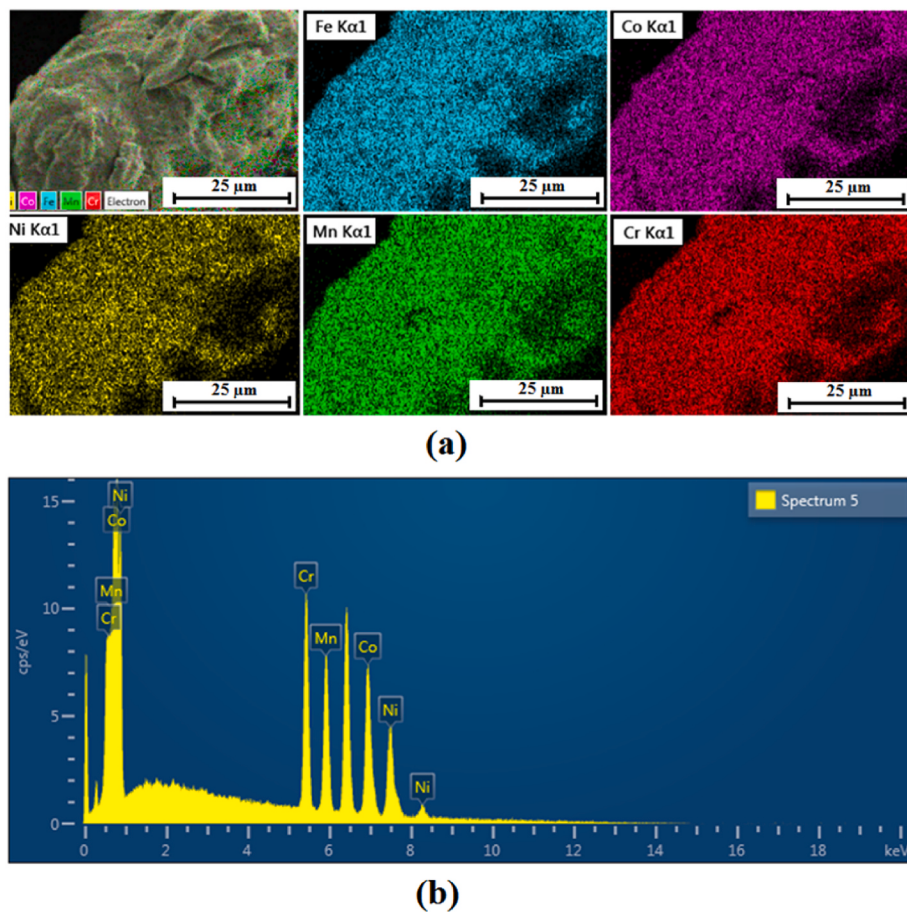


Fig. 6. EDX and elemental mapping of the mechanically alloyed FeCoNiMnCr high entropy alloy.

the vial or milling medium in the as-milled alloy. Fig. 7a shows the magnetic hysteresis loops of the high entropy alloy FeCoNiMnCr measured at 10 K and 300 K. At 10 K and 300 K, the sample does not reach saturation even with an applied 3 T field, exhibiting a paramagnetic response. However, its coercive field at 10 K and 300 K is 550 Oe and 74 Oe, respectively. It's worth mentioning that Zuo et al. [30] found a similar trend with a much greater coercivity of 135 Oe at room temperature. In the presence of a 3 T applied field, the sample exhibits a low magnetization of 5.30 emu/g at 300 K. Ms rises to 22 emu/g at 10 K owing to decreased thermal effects. The temperature dependence of the magnetization recorded in the presence of a 1 T applied field is shown in Fig. 7b. The mean field theory of ferromagnetism [31] explains the reason behind the significant decrement of magnetization as a function of increasing temperature.

3.2. Gamma-ray and neutron shielding properties

In another characterization step of this study, the ionizing gamma-ray and neutron absorption properties of the produced HEA were experimentally investigated. First, the quantitative coefficient values for mass attenuation (μ_m) were measured using experimental techniques. Fig. 8 depicts the fluctuation of μ_m values as a function of ^{133}Ba radioisotope energy. The graph shows that the highest μ_m values are obtained at low gamma-ray energy values. A rapid fall in μ_m values was seen depending on the energy increase. Most low-energy gamma rays are readily absorbed by the HEA attenuator sample positioned between the ^{133}Ba and Ultra High-purity Germanium (HPGe) detector. However, the quantitative increase in gamma-ray energy reduced the quantity of gamma rays absorbed by the HEA attenuator sample. The increased

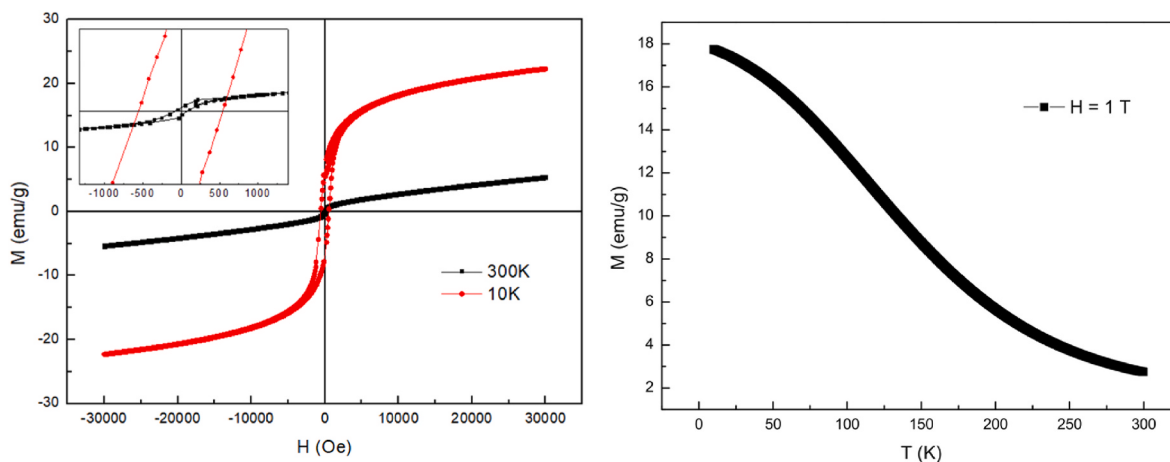


Fig. 7. a) Magnetic hysteresis loops measured at 10 K and 300 K b) M-T curve of FeCoNiMnCr high entropy alloy.

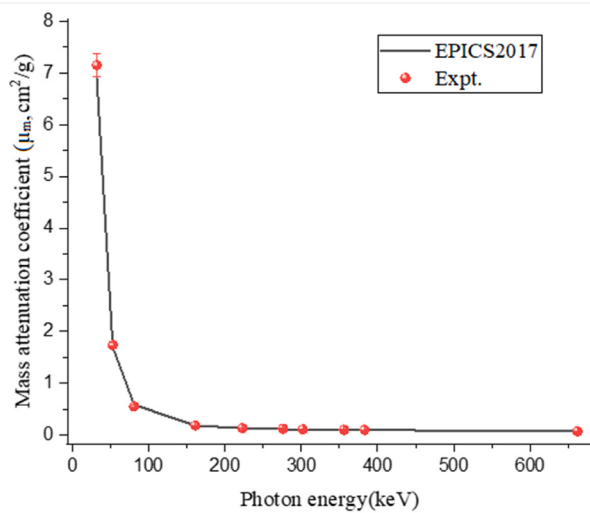


Fig. 8. The variation of mass attenuation coefficient (μ_m) against photon energy for produced HEA alloy.

penetrating capabilities of high-energy gamma rays may explain this. To determine the consistency of the experimentally determined values, we calculated the μ_m values of the HEA sample using the EPICS program [32]. The experimental and theoretical μ_m values and error rates are presented in Table 1. As seen in Table 1, the experimentally determined μ_m values are quite comparable to the EPICS values. The error rates calculated for each energy value are also within the acceptable range.

Table 1
Experimental and theoretical mass attenuation coefficient (MAC) and Half Value Layer (HVL) values of the HEA alloy.

Energy (keV)	MAC (μ_p , cm^2/g)			HVL (cm)	
	EPICS2017 [32]	Expt.	Error	EPICS2017 [32]	Expt.
32	6.9047	7.1526	0.2146	0.0125	0.0121
53	1.6968	1.7365	0.0521	0.0510	0.0498
81	0.5862	0.5524	0.0166	0.1476	0.1567
161	0.1814	0.1845	0.0055	0.4769	0.4690
223	0.1336	0.1321	0.0040	0.6478	0.6549
276	0.1153	0.1210	0.0036	0.7507	0.7152
302	0.1092	0.1095	0.0033	0.7925	0.7903
356	0.0995	0.1015	0.0030	0.8698	0.8526
383	0.0958	0.0978	0.0029	0.9032	0.8848
662	0.0731	0.0712	0.0021	1.1839	1.2149

This quantitative harmony is also a crucial sign of the consistency of the acquired findings and supports the reliability of the experimentally obtained results. On the other hand, HVL value is one of the most practical and application-oriented characteristics that can be determined for shielding material. The physical significance of the HVL value is the material thickness (cm) that can halve the primary gamma ray's intensity, and it may be calculated for the different gamma-ray energies. This study determined the HVL values of the synthesized HEA sample for each gamma-ray energy released by the ^{133}Ba radioisotope. Fig. 9 depicts the fluctuation of HVL values as a function of incident gamma-ray energy values. At low gamma-ray energies, minimal HVL values of HEA were observed. The linear increase in Gamma-ray energy led the way for the increase in HVL values, with the highest gamma-ray energy exhibiting the highest HVL value. Absorption of low-energy gamma rays through attenuation materials may occur at extremely thin thicknesses, which is one of the primary causes of this situation. In a similar manner, the gamma-ray intensity may halve at low material thicknesses. Like the growth in μ_m values, the increase in gamma-ray energy results in a reduction in the quantity of gamma-rays absorbed by the material due to the increase in penetrating qualities. As a result of this situation's impact on the HVL values, a rise in HVL values was observed as the gamma ray energy increased. Although the HEA thickness necessary to reduce by half the intensity of low-energy gamma rays was minimal, the increase in energy required the employment of maximum HEA thicknesses. For example, HVL values were reported as 0.01 cm, 0.05 cm, 0.15 cm, 0.47

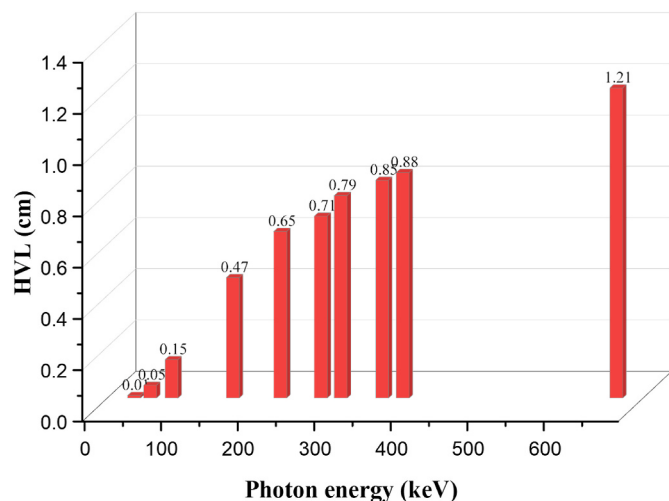


Fig. 9. Variation of half value layer (HVL) against photon energy for the alloy.

cm, 0.65 cm, 0.71 cm, 0.79 cm, 0.85 cm, and 0.88 cm for 53 keV, 81 keV, 161 keV, 223 keV, 276 keV, 302 keV, 356 keV, 383 keV and 662 keV, respectively.

3.3. Benchmarking of gamma-ray and neutron attenuation properties

Comparing the individual attenuation properties of Radiation shielding materials with those of other shields is a crucial step towards a better understanding of shielding properties for practical applications. In the last phase of the current research, gamma-ray and neutron attenuation properties were compared to those of various alloys and neutron absorption materials found in the literature. Fig. 10 depicts the comparison of mean free path (MFP) values of the manufactured HEA sample with Fe20Ni80, Fe86B5C8P1, Inconel 718, 316SS and FeSiMnCrNi alloys reported in the literature [32–36]. Meanwhile, the distance between two consecutive interactions of energetic gamma rays entering the material can be expressed by the MFP values for distinct gamma-ray energies. A low MFP value indicates that the material completes the sequential interactions of gamma-rays at short distances, which is crucial for the material's exceptional gamma-ray absorption capabilities. As seen in Fig. 10, the MFP values of the studied alloys followed almost similar trajectories. The Fe20Ni80 alloy has the lowest MFP values, and the difference with HEA for 4 MeV gamma ray energy is around 0.3 cm. The contribution of the heavy metals in the Fe20Ni80 alloy to the gamma-ray absorption process might explain this disparity. HEA-type alloys have been suggested as the material of choice for future nuclear reactor design, and this issue has been addressed in several earlier papers. This is an essential point that explains the necessity to consider the potential presence of neutron radiation in the environment. Next, the attenuation properties using effective removal cross-section values (Σ_R) of the produced HEA sample against fast neutrons were compared with some conventional neutron absorption materials. Neutrons differ from gamma-rays and X-rays in their interaction with matter due to the neutrality of their electrical charge. For example, electromagnetic radiation types such as gamma rays and X-rays interact with the material primarily at the level of electrons, whereas the situation is different for neutrons. At the level of the nucleus, energetic neutrons interact with materials. Therefore, materials with low atomic weight have a greater tendency to interact with neutrons. Fig. 11 shows the numerical comparison of the Σ_R values of conventional neutron absorbers such as water, graphite, and B₄C with HEA. Apparently, the Σ_R

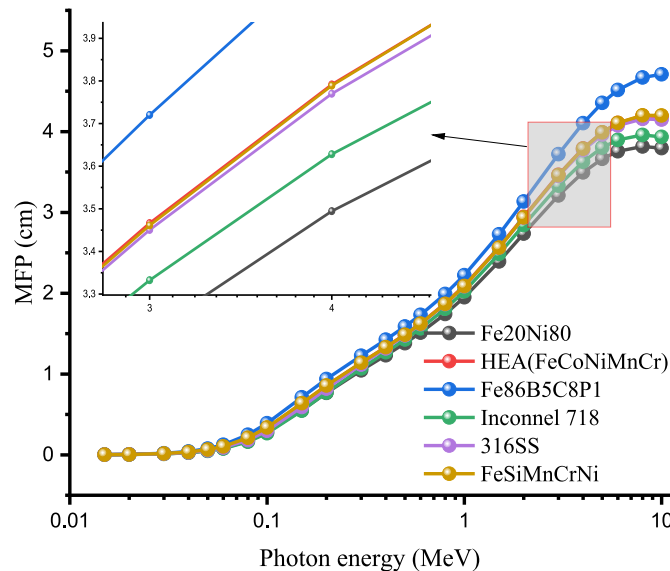


Fig. 10. Variation of mean free path (MFP) against photon energy for the samples.

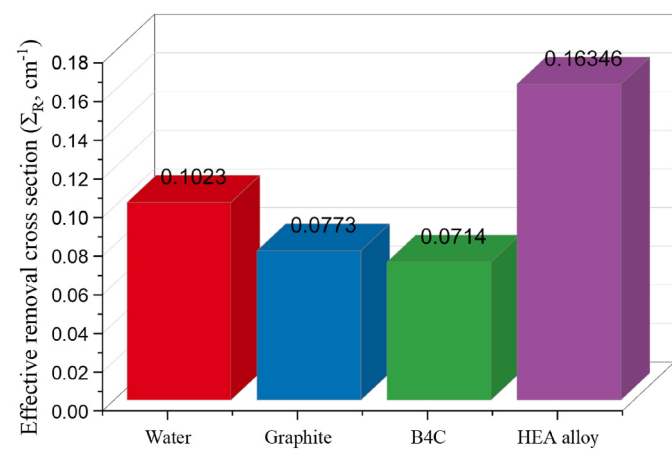


Fig. 11. Comparison of Σ_R values of some neutron absorbers and HEA alloy studied.

value of manufactured HEA is higher than graphite and B₄C. It was also stated that the Σ_R value of HEA was roughly 0.6 cm⁻¹ more than the Σ_R value of water, which is an excellent neutron absorber. This finding demonstrates that the produced HEA is an excellent neutron-absorbing material, and it can be concluded that it may provide an outstanding neutron absorption opportunity in possible applications.

4. Conclusions

The ever-increasing rate of industrialization and the resulting increase in energy consumption and sectoral demands have caused an incredible opportunity to develop targeted and highly efficient energy production techniques. Although energy production based on nuclear reactions is not a new technology, it is a significant scientific method that dynamically covers various technical advancements and rapidly incorporates them into energy production efficiency, material optimizations and, most importantly, nuclear security improvements. The design of nuclear materials and the investigation of their behavioural features is crucial to nuclear technology applications. Recent studies indicate High Entropy Alloys as an acceptable and beneficial material for next-generation nuclear reactors. The primary objective of this research was to investigate some critical material properties of the FeCoNiMnCr HEA sample. According to our findings, FeCoNiMnCr HEA exhibited no major disadvantages. This circumstance served as a significant motivation for the second and primary phase of the study, namely nuclear Radiation shielding properties against gamma-ray and neutrons. For gamma-ray and neutron radiation, the absorption characteristics were examined using experimental and theoretical methods. Overall, an important tendency for gamma ray absorption was found, which was reported at similar values for a variety of alloys based on various chemical configurations investigated in the literature. Notably, the neutron absorption characteristic of the produced FeCoNiMnCr HEA was found to have much greater quantitative values than those of standard neutron moderators, such as water, graphite, and B₄C, which are extensively employed in nuclear reactors. It can be concluded that the newly produced FeCoNiMnCr HEA might be an important candidate for nuclear applications in next-generation nuclear reactors due to its unique and beneficial material and nuclear radiation attenuation properties. In the meantime, this research comprised four phases, including the synthesis phase. Other relevant studies, such as thermal, conductivity, cost analysis, etc., may be conducted in the future to expand the body of knowledge on HEAs, even though the recent findings provide the most crucial behavioral characteristics to the present body of HEA literature.

Funding information

Princess Nourah bint Abdulrahman University Researchers Supporting Project number (**PNURSP2023R149**), Princess Nourah bint Abdulrahman University, Riyadh, Saudi Arabia.

Research data policy

Provided in the manuscript.

Data availability statement

Data is available on request from the authors.

Author contribution: telem simsek

Conceived and designed the analysis, Collected the data, Performed the analysis, Wrote the paper; **Esra Kavaz:** Performed the analysis, Wrote the paper; **Ömer Güler:** Conceived and designed the analysis, Collected the data, Performed the analysis, Wrote the paper; **Tuncay Şimşek:** Contributed data or analysis tools, Collected the data, Performed the analysis; **Başar Avar:** Collected the data, Performed the analysis; **Naim Aslan:** Contributed data or analysis tools, Collected the data, Performed the analysis; **Ghada ALMisned:** Performed the analysis, Wrote the paper; **Hesham M.H. Zakaly:** Performed the analysis, Wrote the paper; **H.O. Tekin:** Performed the analysis, Wrote the paper.

Declaration of competing interest

This manuscript has not been published elsewhere and is not under consideration by another journal.

We have approved the manuscript and agree with submission to **Ceramics International**.

There are no conflicts of interest to declare.

Acknowledgement

The authors would like to express their deepest gratitude to Princess Nourah bint Abdulrahman University Researchers Supporting Project number (**PNURSP2023R149**), Princess Nourah bint Abdulrahman University, Riyadh, Saudi Arabia.

References

- [1] A.O. Moghaddam, et al., Additive manufacturing of high entropy alloys: a practical review, *J. Mater. Sci. Technol.* 77 (2021) 131–162.
- [2] J.W. Yeh, et al., Nanostructured high-entropy alloys with multiple principal elements: novel alloy design concepts and outcomes, *Adv. Eng. Mater.* 6 (5) (2004) 299–303.
- [3] B.S. Murty, et al., *High-entropy Alloys*, Elsevier, 2019.
- [4] E. Pickering, N. Jones, High-entropy alloys: a critical assessment of their founding principles and future prospects, *Int. Mater. Rev.* 61 (3) (2016) 183–202.
- [5] P. Sharma, V. Dwivedi, S.P. Dwivedi, Development of high entropy alloys: a review, *Mater. Today: Proc.* 43 (2021) 502–509.
- [6] Z.U. Arif, et al., Laser deposition of high-entropy alloys: a comprehensive review, *Opt. Laser. Technol.* 145 (2022), 107447.
- [7] Y. Shang, et al., Mechanical behavior of high-entropy alloys: a review, *High-Entropy Mater.: Theory, Exp. Appl.* (2021) 435–522.
- [8] W. Li, et al., Mechanical behavior of high-entropy alloys, *Prog. Mater. Sci.* 118 (2021), 100777.
- [9] Y.-C. Yang, et al., The effect of local atomic configuration in high-entropy alloys on the dislocation behaviors and mechanical properties, *Mater. Sci. Eng.* 815 (2021), 141253.
- [10] R. Motallebi, Z. Savaedi, H. Mirzadeh, Superplasticity of high-entropy alloys: a review, *Arch. Civ. Mech. Eng.* 22 (1) (2022) 1–14.
- [11] V.M. Gopinath, S. Arulvel, A review on the steels, alloys/high entropy alloys, composites and coatings used in high temperature wear applications, *Mater. Today: Proc.* 43 (2021) 817–823.
- [12] A.O. Moghaddam, et al., High temperature oxidation resistance of Al0.25CoCrFeNiMn and Al0.45CoCrFeNiSiO.45 high entropy alloys, *Vacuum* 192 (2021), 110412.
- [13] A.O. Moghaddam, et al., High temperature oxidation resistance of W-containing high entropy alloys, *J. Alloys Compd.* 897 (2022), 162733.
- [14] M.-G. Jo, et al., High temperature tensile and creep properties of CrMnFeCoNi and CrFeCoNi high-entropy alloys, *Mater. Sci. Eng.* (2022), 142748.
- [15] X. Yan, et al., Al0.3CrxFeCoNi high-entropy alloys with high corrosion resistance and good mechanical properties, *J. Alloys Compd.* 860 (2021), 158436.
- [16] K.-M. Hsu, S.-H. Chen, C.-S. Lin, Microstructure and corrosion behavior of FeCrNiCoMnx (x= 1.0, 0.6, 0.3, 0) high entropy alloys in 0.5 M H2SO4, *Corrosion Sci.* 190 (2021), 109694.
- [17] N.J. AbuAlRoos, N.A.B. Amin, R. Zainon, Conventional and new lead-free radiation shielding materials for radiation protection in nuclear medicine: a review, *Radiat. Phys. Chem.* 165 (2019), 108439.
- [18] A. Levet, E. Kavaz, Y. Özdemir, An experimental study on the investigation of nuclear radiation shielding characteristics in iron-boron alloys, *J. Alloys Compd.* 819 (2020), 152946.
- [19] A.H. Almuqrin, et al., Radiation shielding properties of selected alloys using EPICS2017 data library, *Prog. Nucl. Energy* 137 (2021), 103748.
- [20] N. Healey, Lead toxicity, vulnerable subpopulations and emergency preparedness, *Radiat. Protect. Dosim.* 134 (3–4) (2009) 143–151.
- [21] E.J. Pickering, A.W. Carruthers, P.J. Barron, S.C. Middleburgh, D.E.J. Armstrong, A.S. Gandy, High-entropy alloys for advanced nuclear applications, *Entropy* 23 (1) (2021) 98, <https://doi.org/10.3390/e23010098>.
- [22] T. Egami, et al., Local electronic effects and irradiation resistance in high-entropy alloys, *Jom* 67 (10) (2015) 2345–2349.
- [23] S.-q. Xia, et al., Irradiation behavior in high entropy alloys, *J. Iron Steel Res. Int.* 22 (10) (2015) 879–884.
- [24] Y. Zhang, et al., Influence of chemical disorder on energy dissipation and defect evolution in concentrated solid solution alloys, *Nat. Commun.* 6 (1) (2015) 1–9.
- [25] N.K. Kumar, et al., Microstructural stability and mechanical behavior of FeNiMnCr high entropy alloy under ion irradiation, *Acta Mater.* 113 (2016) 230–244.
- [26] G.K. Williamson, W.H. Hall, *Acta Metall.* 1 (1953) 22–31, [https://doi.org/10.1016/0001-6160\(53\)90006-6](https://doi.org/10.1016/0001-6160(53)90006-6).
- [27] Ali Oktay Gul, Esra Kavaz, Oykum Basgoz, Omer Guler, Ghada Almisned, Ersin Bahceci, M. Gokhan Albayrak, H.O. Tekin, Newly synthesized NiCoFeCrW High-Entropy Alloys (HEAs): multiple impacts of B4C additive on structural, mechanical, and nuclear shielding properties, *Intermetallics* 146 (2022), 107593, <https://doi.org/10.1016/j.intermet.2022.107593>.
- [28] C. Suryanarayana, Mechanical alloying and milling, *Prog. Mater. Sci.* 46 (2001) 1–184, [https://doi.org/10.1016/S0079-6425\(99\)00010-9](https://doi.org/10.1016/S0079-6425(99)00010-9).
- [29] T. Simsek, S. Akgül, O. Güler, I. Ozkul, B. Avar, A.K. Chattopadhyay, C.A. Canbay, S.H. Güler, A comparison of magnetic, structural and thermal properties of NiFeCoMo high entropy alloy produced by sequential mechanical alloying versus the alloy produced by conventional mechanical alloying, *Mater. Today Commun.* 29 (2021), 102986, <https://doi.org/10.1016/j.mtcomm.2021.102986>.
- [30] T. Zuo, M.C. Gao, L. Ouyang, X. Yang, Y. Cheng, R. Feng, Y. Zhang, Tailoring magnetic behavior of CoFeMnNiX (X = Al, Cr, Ga, and Sn) high entropy alloys by metal doping, *Acta Mater.* 130 (2017) 10–18, <https://doi.org/10.1016/j.actamat.2017.03.013>.
- [31] J.M.D. Coey, *Magnetism and Magnetic Materials*, Cambridge University Press, 2009, p. 131.
- [32] F.C. Hila, A. Asuncion-Astronomo, C.A.M. Dingle, J.F.M. Jecong, A.M.V. Javier-Hila, M.B.Z. Gili, C.V. Balderas, G.E.P. Lopez, N.R.D. Guillermo, A.V. Amorsolo, EpiXS: a Windows-based program for photon attenuation, dosimetry and shielding based on EPICS2017 (ENDF/B-VIII) and EPDL97 (ENDF/B-VI.8), *Radiat. Phys. Chem.* (2021), 109331, <https://doi.org/10.1016/j.radphyschem.2020.109331>.
- [33] B. Alshahrani, I.O. Olarinoye, C. Mutuwong, Chahkrit Sriwankum, H.A. Yakout, H.O. Tekin, M.S. Al-Buraihi, Amorphous alloys with high Fe content for Radiation shielding applications, *Radiat. Phys. Chem.* 183 (2021), 109386, <https://doi.org/10.1016/j.radphyschem.2021.109386>.
- [34] Bünyamin Aygün, Neutron and gamma radiation shielding Ni based new type super alloys development and production by Monte Carlo Simulation technique, *Radiat. Phys. Chem.* 188 (2021), 109630, <https://doi.org/10.1016/j.radphyschem.2021.109630>.
- [35] Uğur Gökmen, Gamma and neutron shielding properties of B4C particle reinforced Inconel 718 composites, *Nucl. Eng. Technol.* 54 (2022) 1049–1061, <https://doi.org/10.1016/j.net.2021.09.028>.
- [36] Jamila S. Alzahrani, Z.A. Alrowaili, Canel Eke, M. Zakaria, M. Mahmoud, C. Mutuwong, M.S. Al-Buraihi, Nuclear shielding properties of Ni-, Fe-, Pb-, and W-based alloys, *Radiat. Phys. Chem.* 195 (2022), 110090, <https://doi.org/10.1016/j.radphyschem.2022.110090>.